Ecosystems (2005) 8: 17–32
DOI: 10.1007/s10021-004-0027-9

ECOSYSTEMS

Tree Canopy Effects on Simulated Water Stress in Southern African Savannas

Kelly K. Caylor,[1]* Herman H. Shugart,[2] and Ignacio Rodriguez-Iturbe[1]

[1]*Department of Civil and Environmental Engineering, Princeton University, Princeton, New Jersey 08540, USA;* [2]*Department of Environmental Sciences, University of Virginia, Charlottesville, Virginia 22904, USA*

Abstract

A coupled energy and water balance model is used to simulate the effects of large tree canopies on soil moisture and water stress across a series of sites spanning a regional moisture gradient in southern Africa. The model tracks evapotranspiration from five components of the land surface at each site—the tree canopy, the grass under and between tree canopies, and the bare soil under and between tree canopies. The soil moisture dynamics are simulated at daily time steps and driven by a stochastic model of storm arrivals and storm depth. Evapotranspiration is modeled using the Priestley-Taylor approach, with potential evapotranspiration scaled by soil moisture availability. The soil moisture under tree canopies is compared to the soil moisture between tree canopies, and differences in average annual soil moisture stress conditions are analyzed at each site. The spatial distribution of large trees has important consequences for small-scale soil moisture dynamics across the rainfall gradient. The results indicate that tree canopies serve to reduce soil moisture stress of under-canopy vegetation in the middle of the rainfall gradient. At the dry end of the rainfall gradient, the effect of tree canopies on soil moisture is dependent on the amount of rainfall received in a given growing season.

Key words: energy and water balance model; tree canopies; soil moisture; water stress; rainfall; southern Africa; Kalahari Transect.

Introduction

Savannas have been variously defined, but they are generally described as mixed life-form vegetation communities in which woody and herbaceous components codominate (Bourliere and Hadley 1970; Walter 1971; Sarmiento 1984; Tothill and Mott 1985). In addition to their characteristic structural heterogeneity, savannas typically experience strong seasonality in rainfall, with pronounced wet and dry seasons and a high degree of interannual variability in rainfall (Huntley and Walker 1982). The conspicuous shared dominance of contrasting plant life-forms makes savannas inherently interesting from an ecological perspective; moreover, their geographic and socioeconomic importance is underscored by the rapid growth in human populations that depend on these lands for wood products and livestock rangeland. Tropical savannas are distributed over an eighth of the terrestrial surface and make up one-half of African land cover (Atjay and others 1987).

This paper describes the development and application of a model of the daily water and energy balance of each component of the savanna landscape at a set of research sites, collectively called the Kalahari Transect. The Kalahari Transect, one of a number of International Geosphere-Biosphere Programme (IGBP) transects designated throughout the world (Koch and others 1995),

Received 28 February 2003; accepted 12 September 2003; published online 7 January 2005.
*Corresponding author; e-mail: kcaylor@princeton.edu

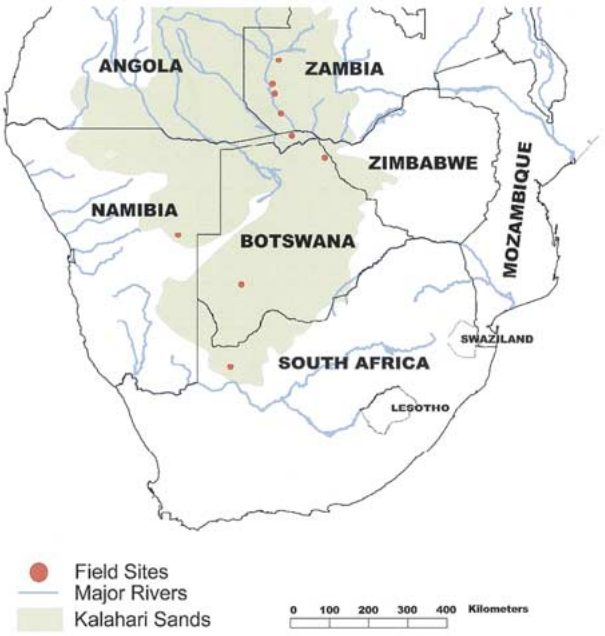

Figure 1. Distribution of Kalahari sands and major rivers in southern Africa. Locations of sites used in this study are also provided.

covers a latitudinal mean annual precipitation (MAP) gradient ranging from 1,000 mm/y in the north to 250 mm/y in the south. Figure 1 shows the location of the research sites used in this study. The rainfall gradient across these sites (Table 1) results in dramatic variation in vegetation structure along the transect (Scholes and others 2002; Caylor and others 2003; Privette and others 2004). These structural variations, coupled with the regional rainfall gradient, lead to changes in the relative contribution of trees and grasses to vegetation productivity across the transect (Dowty and others 2000; Caylor and others 2004). Consistency in geomorphology over the entire region—primarily deep Kalahari sands (Thomas and Shaw 1991)—allows for an analysis of vegetation structure and ecosystem processes that is relatively independent of soil type.

Our aim in this paper is to explore a vexing problem in vegetation science—the underlying causes of the factors that allow savanna vegetation to persist as a mixture of grasses and trees. The shared dominance among tree and graminoid life-forms across vast regions in the semi-arid tropics and subtropics (and more widely under expansive definitions of savanna) is surprising. One might expect a particular life-form to be best adapted and most successful in a particular environment. Not only do trees and grasses differ in physiognomy and life history, but in the case of African savannas the trees use the C3 photosynthetic pathway whereas the grasses are typically C4 species. This physiological differentiation implies a greater likelihood of niche differentiation. The extensive distribution of savannas worldwide suggests that they are not a knife-edge case where environmental conditions favoring tree dominance transition to conditions favoring grass dominance (Jeltsch and others 2000).

Our conclusion from investigating a model of coupled water and energy balance applied to savannas is that, along realistic environmental gradients, the biophysics of tree and grass canopy performance result in competitive tree–grass interactions in both moist and dry conditions and mutualistic interactions in intermediate conditions. We address these interactions as a consequence of the contrasting microclimates under and between tree canopies across the Kalahari Transect using a simple coupled energy and water balance model that treats under-canopy and between-canopy environments as discrete spatial units with separate energy and water balance. Model behavior is explored at nine locations where necessary structural data are available for model parameterization. These investigations reveal a complex pattern of tradeoffs between light and moisture availability both across the rainfall gradient and within a single site.

Grass–Tree Interactions in African Savanna Ecosystems

In southern Africa, tropical savannas are extensive but varied, ranging from partially closed woodlands to sparsely covered scrublands (Scholes and Walker 1993). Many tropical savannas are found in semi-arid climates where a constantly changing distribution of soil moisture is supplied by predominantly convective storms that vary considerably in both frequency and depth (McCown and Williams 1990; Sala and Laurenroth 1982; Hutley and others 2001). The importance of water limitation in savannas has spawned different theoretical models of tree–grass coexistence. These models differ in their underlying assumptions about the ways in which trees and grasses access and use soil moisture. Walter (1971) proposed a spatial niche-differentiation model to explain a balance of trees and grasses at equilibrium. This model was based on the idea that tree and grass roots use different soil layers for their water supplies—trees having deep roots and grasses having shallower roots. However, due to a lack of direct evidence of a two-tiered

Table 1. Site Locations, Description, and Vegetation Structural Parameters Used in the Coupled Energy/Water Balance Model LAI_t, tree canopy leaf area index (m^2 m^{-2}); f_c, fraction of tree canopy cover

Site	Latitude	Longitude	Vegetation Type	Annual Precip (mm)[a]	LAI_t[b]	f_c[b]	LAI_g[b]	f_g
Lishuwa Communal Forest (Lukulu, Zambia)	14.42S	23.52E	Evergreen woodland	970	5.53	0.844	0.35	.10
Kataba Forest Reserve (Mongu, Zambia)	15.44S	23.25E	Kalahari woodland	879	2.47	0.648	0.38	.20
Liangati Forest Reserve (Senanga, Zambia)	15.86S	23.34E	Kalahari woodland	811	2.52	0.537	1.1	.30
Maziba Bay Forest (Sioma, Zambia)	16.75S	23.61E	Dry Kalahari woodland	737	2.08	0.610	0.81	.30
Sachinga Agricultural Station (Katima Mulilo, Namibia)	17.70S	24.08E	Combretum woodland	707	1.16	0.299	2.1	.50
Pandamatenga Agricultural Station (Pandamatenga, Botswana)	18.66S	25.50E	Schinziophyton, Baikiaea, Burkea woodland	698	2.04	0.323	1.4	.50
Sandveld Research Station (Gobabis, Namibia)	22.02S	19.17 E	Acacia–Terminalia woodland	409	.69	0.191	1.4	.30
Tshane (Tshane, Botswana)	24.17S	21.89E	Open Acacia savanna	365	.61	0.321	0.87	.30
Vastrap Weapons Range (Upington, South Africa)	27.75S	21.42E	Open Acacia shrubland	216	.35	0.058	0.80	.20

[a] *Annual precipitation derived from station data. Station information provided in Scholes and others (2002).*
[b] *Canopy cover determined from field observations (Caylor and others, 2003). LAI determined from canopy observations (Caylor and others 2003). Allometric relationships derived from Goodman (1990), as modified by Dowty (1999).*
[c] *Grass cover determined from 1-m quadrat samples taken at each site during peak growing season as described by Scholes and others (2002). Grass LAI determined from grass biomass (g/m^2 -ground) and specific leaf area (m^2 -leaf/g). LAI_g leaf area of grass vegetation (m^2 ma^{-2}); and f_g, fraction of grass vegetation cover*

layering of root structure in many savanna environments, the validity of this hypothesis has been questioned (Fisher and others 1994; Knoop and Walker 1985; Hipondoka and others 2003). Accordingly, the Walter model has been modified in a number of ways to better approximate field observations (see Scholes and Archer 1997 for an excellent review).

Several studies have investigated the effect of tree canopies on various components of soil water balance. Site-level observations have shown an increase in soil moisture storage and drainage under tree canopies (Joffre and Rambal 1993), a decrease in the duration of soil wetness and reduced soil water content between tree canopies (Breshears and others 1997, 1998), and strong gradients in light, temperature, and soil moisture from under-canopy to between-canopy environments (Belsky and others 1989). Differences in canopy microclimate have been shown to lead to higher productivity of grass under trees in a low-rainfall savanna, but a lower relative productivity of under-canopy grasses in a high-rainfall savanna (Belsky and others 1993). More recently, Jackson and Wallace (1999) described a reduction of as much as 40% in bare soil evaporation under tree canopies in a Kenyan agro-forestry plantation, and Smit and Rethman (2000) report increased infiltration and evapotranspiration in experimentally thinned plots of Mopane woodland (*Hardwikia mopane*). Differences in soil moisture under and between tree canopies have been used to explain observed patterns of herbaceous productivity in humid west African savannas (Menaut and Cesar 1979; Mordelet and Menaut 1995). Soil moisture has also been seen, to impact seedling germination of southern African woody vegetation (Keya 1997; Wilson and Witkowski 1998) and the distribution patterns of woody species (Smith and Grant 1986; Smith and Goodman 1987).

Models of Savanna Grass–Tree Interactions

Despite observations of the effects of tree canopies in savannas, the inclusion of horizontal spatial processes in models of savanna dynamics is relatively recent (Jeltsch and others 1998). Initial dynamic models of tree–grass coexistence assumed that soil moisture is horizontally homogeneous (Eagleson and Segarra 1985) and that competition for soil moisture is sufficient to explain observed patterns of uniform vegetation spacing in semi-arid systems (Yeaton and Cody 1976; Phillips and MacMahon 1981). Subsequent field studies of southern African savanna spatial pattern (Skarpe 1990; Jeltsch and others 1996) have shown that uniform patterns in savanna vegetation are not as common as first thought. In addition, a recent survey of vegetation pattern at 10 sites across the Kalahari Transect rainfall gradient (Caylor and others 2003) found that the aggregation of juvenile woody vegetation was significantly influenced by the distribution of large tree canopies at six of 10 sites. These results suggest that patterns of woody vegetation structure are controlled by the distribution of favorable sites for juvenile establishment.

The observation of complex, nonuniform distributions of vegetation and the influence of trees on under-canopy microclimate have led to models of savanna dynamics and productivity that explicitly include horizontal processes. These models incorporate spatial processes either through landscape-scale spatial heterogeneity (Coughenour 1992), grid-based cell automata (Gignoux and others 1995; Jeltsch and others 1998), individual interactions (Lonsdale and others 1998; Simioni and others 2000), or patch-scale structural parameterization (Caylor and others 2004). Most promisingly, Breshears and Barnes (1999) have proposed a unifying conceptual model that incorporates both horizontal patchy vegetation structure and vertical distributions of root profiles.

A Coupled Water and Energy Balance Model

Our model links the daily water and energy balance of each component of the savanna landscape during the wet season through the effects of net radiation and soil moisture on rates of latent energy transfer. It resolves net radiation and latent heat flux for five separate components of the land surface—tree canopy (denoted $X_{(t,c)}$ when referring to components of a flux), grass under canopy ($X_{(g,c)}$), grass between canopies ($X_{(g,b)}$), bare soil under canopy ($X_{(s,c)}$), and bare soil between canopies ($X_{(s,b)}$). $X_{(x,y)}$ refers to any component of the land surface in general formulations. All fluxes are in dimensions of W m^{-2}. The fraction of area covered by trees is denoted f_c, the grasses is denoted f_g. Grasses are assumed to be distributed evenly between and under tree canopies, so that the fraction of bare soil is $(1 - f_g)$.

Evapotranspiration is characterized by the Priestley-Taylor approximation, which infers rates of latent energy transfer as a function of atmospheric demand. The relative components are resolved into canopy (X_c) and between-canopy (X_b)

Table 2. Parameters, Parameter Values, and Reference Sources Used in the Coupled Energy/Water Balance Model

Parameter	Value(s)	Reference
α_g,α_t	0.20,0.25	Campbell and Norman (1998)
α_s	0.35	
e_s	0.95	
k_s	0.35	Brutsaert (1982)
s_*^t	0.12	Scholes and Walker (1993); Laio and others, (2001); Porporato and others, (2003)
s_*^g	0.17	
s_{wt}	0.05	
s_{wg}	0.06	
s_{sat}	0.40	
s_h	0.03	
Z_R	1,000 mm	
n	0.40	
q	2	
a_1	−2.1154	Data from Scanlon and Albertson (2004)
a_2	0.0108	
a_3	1.0029	
b_1	2.0850	
b_2	0.0005	
b_3	0.0425	

by summing the component fluxes according to $X_c = X_{(s,c)} + X_{(g,c)} + X_{(t,c)}$ and $X_b = X_{(s,b)} + X_{(g,b)}$. The weighted scalar value of the flux X for the entire landscape is then $X = (1 - f_c)X_b + f_cX_c$. The derivation of each component of the energy balance is provided in the following subsections. Values of parameters referred to in the model description are provided in Tables 1 and 2.

Shortwave Radiation

Average daytime incoming solar radiation (S_{sky}) is determined based on an 8-year average of the monthly mean solar radiation $\overline{S_{sky}}$ provided by the NASA (Darnell and others 1996). The global 1-degree data is subsetted to include only the Kalahari Transect, defined as 14°S to 27°S at 25°E. The monthly $\overline{S_{sky}}$ at each site is determined using the 1-degree data corresponding to the site's latitude. For each day, the average daytime incoming radiation is the monthly value of $\overline{S_{sky}}$ multiplied by the 24 h in a day and divided by the number of daylight hours in the day (h_{day}), the latter a function of Julian day and latitude (Campbell and Norman, 1998). Incident shortwave radiation upon the tree canopy is $S_{d(t,c)} = S_{sky}[1-\exp(-k_sLAI_t)]$, where k_s is the extinction coefficient of shortwave radiation and LAI_t is the leaf area index of the tree canopy [m^2 m^{-2}]. Net radiation upon the tree canopy is $S_{n(t,c)} = (1-\alpha_c)S_{d(t,c)}$, where α_c is the tree canopy shortwave albedo and shortwave incoming radiation available under the tree canopy is $S_{dwn} = S_{sky}-S_{d(t,c)}$. Net shortwave radiation for under canopy grasses ($S_{n(g,c)}$) and under-canopy bare soil ($S_{n(s,c)}$) are $S_{n(g,c)} = f_g[S_{dwn}(1 - \alpha_g)]$ and $S_{n(s,c)} = (1 - f_g)[S_{dwn}(1 - \alpha_S)]$, where α_g and α_s, are the shortwave albedos for the grass canopy and bare soil, respectively. Net shortwave radiation upon the between canopy grass is $S_{n(g,b)} = f_g[S_{sky}(1 - \alpha_g)]$, and net shortwave radiation upon the between-canopy bare soil is $S_{n(s,b)} = (1 - f_g)[S_{sky}(1 - \alpha_s)]$.

Longwave Radiation

Incoming longwave radiation is given as $L_{sky} = e_a\sigma T_a^4$, where σ is the Stefan-Boltzmann constant, T_a is the atmospheric temperature in degrees Kelvin at reference height (taken to be 10 m), and $e_a = 9.2 \times 10^{-6}T_a^2$ is the atmospheric emissivity, determined from Brutsaert (1982). The annual pattern of mean daily air temperature is modeled using a coarse-scale empirical model of mean temperature derived specifically for the Kalahari region. For this study, stochastic variation in mean daily temperature is ignored, and an empirically derived 5th-degree polynomial approximation of average daily temperature is used in the absence of appropriate station data. A 2-year record of daily meteorological data reported in Dowty and other (2000) is used to determine the coefficients of the 5th-degree polynomials describing daily mean temperature at 4 sites within the Kalahari region. The relationship between (MAP) and polynomial coefficients at these sites yields a criterion for determining polynomial coefficients for locations where daily meteorological data are unavailable, but MAP is known. This methodology allows for a simple approximation of the climatological mean daily patterns of temperature for any location along the rainfall gradient.

Soil temperature is modeled using two different empirical relationships developed from a series of diurnal half-hourly meteorological measurements taken at three sites across the rainfall gradient (Scanlon and Albertson, 2004). At each site, bare soil observations of soil surface temperature for both vegetated and unvegetated areas were monitored, along with concurrent observations of sur-

face energy balance and microclimatological data. Soil temperature between the tree canopies showed an exponential relationship with shortwave radiation and air temperature, whereas soil temperature under the canopies had a linear relationship to these two variables. Therefore, both between-canopy soil temperature ($T_{(s,b)}$) and under canopy soil temperature ($T_{(s,c)}$) are functions of air temperature and incoming shortwave radiation as $T_{(s,b)} = \exp(b_1 + b_2 S_{sky} + b_3 T_a)$ and $T_{(s,c)} = a_1 + a_2 S_{dwn} + a_3 T_a$, where a_i and b_i are empirical coefficients derived from the ensemble of daytime observations (Table 2).

Each of the soil temperature models has a high degree of correlation with the observed data (under-canopy: $r^2 = 0.85$, $P < 0.001$; between canopy: $r^2 = 0.80$, $P < 0.001$) across a wide range of soil temperatures. When bare soil temperature is higher than 45°C, the model consistently predicts lower temperatures than are observed. This bias does not affect the modeling exercise presented here because average daily bare soil temperatures do not exceed 35°C. All vegetation components are assumed to be in thermal equilibrium with the atmosphere during the daytime so, that $L_n = 0$ for all vegetation components and $T_{(t,c)} = T_{(g,c)} = T_{(g,b)} = T_a$. Outgoing longwave radiation for each of the two soil components ($L_{(s,c)}$, $L_{(s,b)}$) is given as $L_{(s,c)} = (1 - f_g) e_s \sigma T_{(s,c)}^4$, and $L_{(s,b)} = (1 - f_g) e_s \sigma T_{(s,b)}^4$, where e_s is the thermal emissivity of soil. Net longwave radiation [W m^{-2}] for the bare soil under tree canopy ($L_{n(s,c)}$) and bare soil between canopies ($L_{n(s,b)}$) is then given as $L_{n(s,c)} = (1 - f_g) L_{sky} - L_{(s,c)}$ and $L_{n(s,b)} = (1 - f_g) L_{sky} - L_{(s,b)}$.

Net Radiation and Available Radiation

A key model assumption is that the atmosphere is well mixed with respect to the various components of the landscape. Therefore differences in soil temperature do not lead to differences in air temperature under and between canopies, and we ascribe a single daily mean temperature to each. Although we expect that there will be some coupling between the land surface and the turbulent boundary layer air properties (for example, Scanlon and Albertson, 2003), such coupling is likely to occur at time and space scales that are incompatible with our approach. The net radiation (R_n,) for each landscape component is defined as $R_n = L_n + S_n$. The Priestley-Taylor estimations of evaporation and transpiration depend on the quantity of energy available, Q. For the two soil components, available energy is given by $Q_{soil} = (1 - C_G) R_n$, where C_G is the ground flux coefficient taken to be 0.3 (compare Lhomme and Monteny 2000). The value of C_G varies with soil moisture across a range of 0.2–0.6 (Idso and others 1975) due to the changing thermal diffusivity of the soil as the water content increases and decreases through time (Brutsaert 1982). However, the use of a constant value of C_G that falls in the middle of the observed range (Choudhury and others 1987) is reasonable assumption (compare Kustas and Norman 1997), particularly because differences caused by variation in C_G are small compared to the variability in net radiation driven by the differences in T_c and T_b. Available energy for the three vegetation components is given by $Q_{veg} = R_n - D_{veg}\lambda_{veg}$, where $D_{veg}\lambda_{veg}$ is the latent energy used to evaporate intercepted water in each vegetation component. The determination of D_{veg} is presented in the water balance section.

Latent Heat Flux

Latent heat flux is determined using a Priestley-Taylor potential evaporation approach scaled to take into account soil moisture availability. The determination of potential evaporation using the Priestley-Taylor formulation is given by:

$$PET_{PT} \equiv \frac{\alpha \Delta}{\Delta + \gamma} Q,$$

where α is the Priestley-Taylor coefficient, generally taken to be 1.26; and γ is the psychrometric constant [Pa/K], which is derived from atmospheric pressure (P_{atm}, [Pa]), heat capacity (C_p [J kg^{-1} K^{-1}]), and latent heat of vaporization (λ [J kg^{-1}]) according to:

$$\gamma = \frac{P_{atm} \cdot C_p}{0.622\lambda}.$$

At each site, P_{atm} was determined from site elevation (h_e, [m]) using:

$$P_{atm} = 101325 \left(\frac{288 - .0065 \cdot h_e}{288} \right)^{5.256}.$$

The final term in the Priestley-Taylor equation, Δ, is the derivative of the relationship between saturation vapor pressure and air temperature [Pa/K] approximated by $\Delta = 48.7 \cdot \exp(8.2647 e^{-3} \cdot T_a)$. The limitation of transpiration by soil moisture over vegetated surfaces follows an approach developed by Rodriguez-Iturbe and others (1999) and is given by:

$$\tau(s) = \begin{cases} s < s^* & \tau = \frac{s - s_w}{s^* - s_w} \\ s \geq s^* & \tau = 1 \end{cases}$$

where s is the relative soil moisture expressed as the ratio of volumetric soil moisture to porosity, s^*

is the vegetation specific relative soil moisture above which plants experience unstressed transpiration, and s_w is the vegetation-specific wilting point at which point transpiration ceases (Table 2). When determining $\tau(s)$ for each component of the vegetation, trees are assumed to experience the mean landscape soil moisture, s, whereas grass under the canopy and grass between canopies experience the local soil moisture, s_c and s_b, respectively. The resulting linear scaling coefficient is used to determine LE for each vegetation component according to:

$$LE_{veg} = \frac{\alpha\Delta}{\Delta+\gamma} Q_{veg}\tau(s).$$

Limitation of potential bare soil evaporation uses an exponential β-function approach, modified from the presentation of Boulet and others (2000) to scale PET_{PT} by the difference between the actual and saturated soil water content $\beta(s) = \exp(-k(1-s))$, where k is a coefficient of limitation. The coefficient k is set so that bare soil evaporation is approximately zero when relative soil moisture reaches the hygroscopic point, s_h, given as $s_h = 0.03$ for the sandy soils studied here. Therefore, we assign $k = 10$, so that $\beta(s_h) = 6 \times 10^{-5}$. Latent heat flux for each soil component is then determined according to:

$$LE_{soil} = \frac{\alpha\Delta}{\Delta+\gamma} Q_{soil}\beta(s)$$

Water Balance

Three representations of the soil moisture balance in a given landscape are monitored: the relative soil moisture under tree canopies (s_c), the relative soil moisture between tree canopies (s_b), and the weighted average relative soil moisture of the landscape (s); s is given by $s = (1 - f_c)s_h + f_c s_c$ where f_c is the fraction of the landscape covered by tree canopies, defined from field data. The daily change in each component of the soil moisture [mm] is given by:

$$nZ_R \frac{ds_c}{dt} = I_c - E_c - L_c$$

and

$$nZ_R \frac{ds_b}{dt} = I_b - E_b - L_b$$

where n is soil porosity and Z_R [mm] is the effective rooting depth of the soil. Rates of inputs and losses vary independently for each soil moisture component, so that I_c and I_b are the infiltration rates for the canopy and between-canopy components, respectively [mm d^{-1}]; E_c and E_b are the component-specific losses through evapotranspiration [mm d^{-1}]; and L_c and L_b are the canopy and between-canopy losses due to drainage below the rooting depth [mm d^{-1}].

Daily rainfall h [mm] is partially intercepted by both the tree and grass canopies. Tree canopy interception h_*^t [mm] is taken to be a constant 2 mm, and grass interception (h_*^g) is taken to be a constant 1 mm (Scholes and Walker 1993). The minimum storm depth necessary to generate infiltration below the tree canopy (h_*^c) and between the canopies h^*_b is then $h_*^c = h_*^t + f_g h_*^g$, and $h_*^b = h + f_g h_*^g$. The total amount of intercepted water is assumed to evaporate from trees and grasses (D_t and D_g, respectively [mm s^{-1}]) during the day and is given by $D_{veg} = D_t + D_g$, where:

$$D_t = \frac{\min(h, h_t^*)}{3600 \cdot h_{day}}$$

and

$$D_g = \frac{\min(h, h_g^*)}{3600 \cdot h_{day}}$$

Rainfall in excess of h^* is available for infiltration. Infiltration is limited by soil porosity and the current soil moisture in each component of the landscape according to:

$$I_c = if(h - h_c^*) > 0, \min\begin{bmatrix} h - h_c^* \\ nZ_R(1 - s_c) \end{bmatrix}$$

and

$$I_b = if(h - h_b^*) > 0, \min\begin{bmatrix} h - h_b^* \\ nZ_R(1 - s_b) \end{bmatrix}$$

and

$$I = f_c I_c + (1 - f_c) I_b$$

Tree canopy transpiration is assumed to draw from both the under-canopy and between-canopy soil reservoirs, whereas the transpiration of under-canopy and between-canopy grasses is localized to s_c and s_b, respectively. Loss due to tree canopy transpiration from each of the two reservoirs is further constrained by the relative plant-available moisture in each reservoir (PAM_c and PAM_b), defined as:

$$PAM_c = \begin{cases} s_c > s_{wt} & \frac{s_c - s_{wt}}{(s_c + s_b) - 2s_{wt}} \\ s_c \leq s_{wt} & 0 \end{cases}$$

and

$$PAM_b = \begin{cases} s_b > s_{wt} & \frac{s_b - s_{wt}}{(s_c + s_b) - 2s_{wt}} \\ s_b \leq s_{wt} & 0 \end{cases}$$

where s_{wt} is the wilting point for trees. The total evapotranspiration [mm d^{-1}] from the canopy portion of the landscape is given by:

$$E_c = \left(\frac{LE_{(s,c)}}{\lambda_{(s,c)}} + \frac{LE_{(g,c)}}{\lambda_{(g,c)}} + PAM_c \cdot \frac{LE_{(t,c)}}{\lambda_{(t,c)}} \right) \cdot 3600 \cdot h_{day},$$

where λ is the latent heat of vaporization [W mm^{-1}] for each component and is determined according to $\lambda = 3.1512 \times 10^6 - 2.38 \times 10^3 \, T$, where T is the temperature of the evaporating surface in degrees kelvin. Evapotranspiration from between-canopy areas [mm d^{-1}] is calculated using:

$$E_b = \left(\frac{LE_{(s,b)}}{\lambda_{(s,b)}} + \frac{LE_{(g,b)}}{\lambda_{(g,b)}} + PAM_b \cdot \frac{LE_{(t,c)}}{\lambda_{(t,c)}} \right) \cdot 3600 \cdot h_{day},$$

Finally, total evapotranspiration [mm d^{-1}] is weighted by the fraction of canopy (f_c) and between canopy ($1 - f_c$) portions of the landscape and is given as $E = (1 - f_c)E_b + f_c E_c$.

At daily time scales in coarsely drained soils, and assuming no interaction with underlying soil layers, excess moisture in the soil reservoir is assumed to drain to field capacity. Therefore, drainage below rooting depth for the canopy, between-canopy, and total landscape (L_c, L_b, and L, respectively [mm]) are determined according to:

$$L_c = (s_c - s_{fc}) n Z_R \quad if \; s_c > s_{fc}$$

$$L_b = (s_b - s_{fc}) n Z_R \quad if \; s_b > s_{fc}$$

$$L = (1 - f_c) L_b + f_c L_c$$

Water Stress

Water stress in each vegetation component (x,y) within the landscape is characterized using the static moisture stress, ς, generally defined by Porporato and others (2001) as:

$$\varsigma_{(x,y)} = \left[\frac{s^* - s}{s^* - s_w} \right]^q$$

where s^*, s_w, and s are defined in the preceding section on latent heat flux; and q is a parameter that denotes the nonlinear nature of soil water deficit on plant stress, taken to be 2 (Porporato and others 2001). For each day, the daily static stress of each vegetation component ($\varsigma_{(t,c)}$, $\varsigma_{(g,c)}$, and $\varsigma_{(g,h)}$) is found using the vegetation-specific s^* (s_t^* or s_g^*), the wilting point (s_{wt} or s_{wg}), and the appropriate soil moisture value (s_c, s_b, or s). To assess the potential water stress of juvenile woody vegetation (that is, subcanopy trees and shrubs), we also define $\varsigma_{(jt,b)}$ and $\varsigma_{(jt,c)}$, which are simply the static stress that would be experienced by juvenile tree vegetation growing in the between-canopy and under-canopy environments, respectively, assuming the same wilting point threshold as mature trees. As opposed to the mature trees (that is, canopy dominant vegetation) that experience the landscape average soil moisture, the juvenile tree only vegetation experiences only the local soil moisture (s_c or s_b). Therefore, although we do not consider the structure of small trees and shrubs directly within the model, this formulation enables a comparison of the potential water stress that may be experienced by small trees (that is, subcanopy juveniles) growing either under or between large tree canopies (that is, canopy-dominant adults). Cumulative stress, ϕ is indexed as the number of days, t, during which ς is greater than 0 for each vegetation component (x,y) as:

$$\phi_{(x,y)} = \sum_{t=1}^{n} \begin{Bmatrix} 1 & \varsigma_{(x,y)}(t) > 0 \\ 0 & \varsigma_{(x,y)}(t) = 0 \end{Bmatrix}.$$

The ratio of cumulative stress for the under- and between-canopy portions of the landscape is used as a measure of the different effect of water availability on plant–water relations and stress between these two portions of the landscape.

Site Parameterization and Simulation

The scarcity of long-term daily rainfall data for many areas of the Kalahari Transect necessitates the use of stochastic modeling techniques to infer rainfall patterns in areas where stations are not temporally or spatially extensive. Recent work by Porporato and others (2003) has analyzed 25+ years of daily rainfall data for a series of sites across the Kalahari Transect. They find that the stochastic model described by Rodriguez-Iturbe and others (1999) is an appropriate description of the distribution of growing season rainfall for the Kalahari region. Accordingly, rainfall is simulated using a stochastic model based on a poisson distribution of storm arrivals and an exponential distribution of

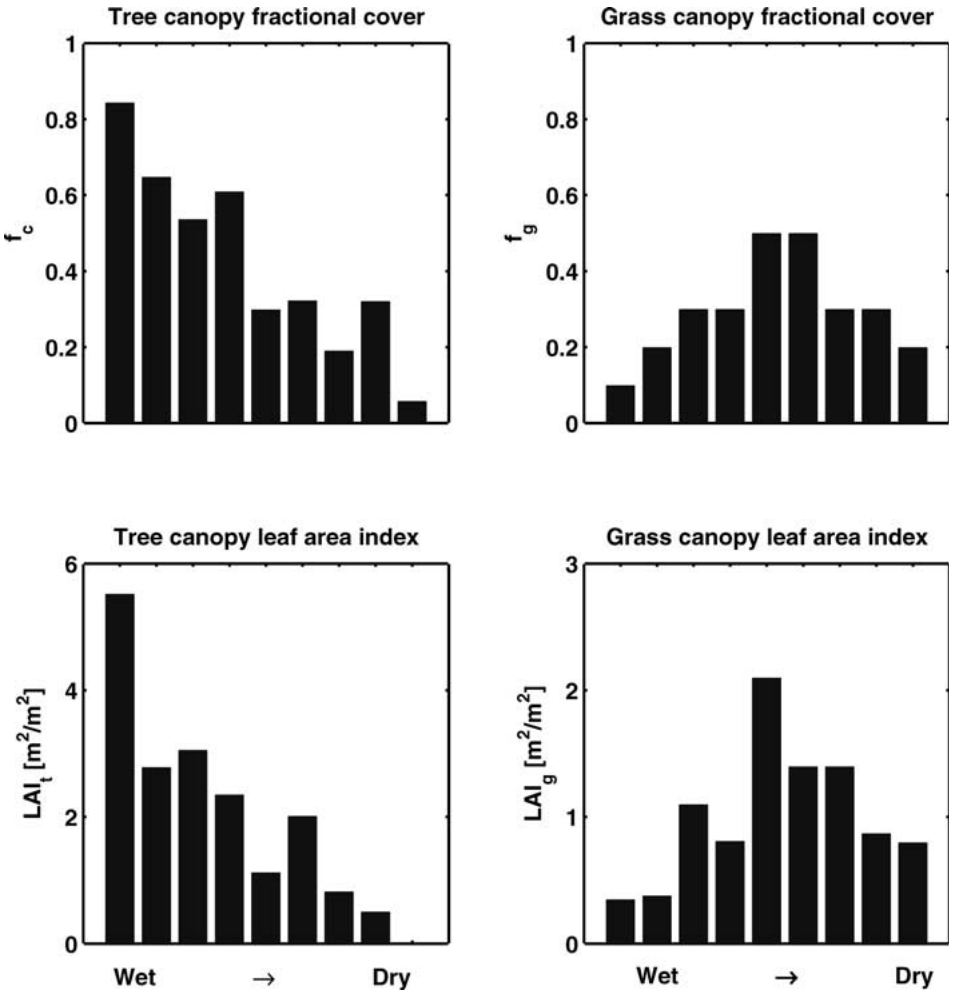

Figure 2. Vegetation structural characteristics at each site along the Kalahari Transect. Within each graph, the sites proceed from left to right along decreasing latitude and mean annual rainfall. Tree leaf area index (LAI_t) and tree fractional cover (f_c) decrease with rainfall, while grass fractional cover (f_g) and grass leaf area index (LAI_g) reach a peak in the middle of the transect.

storm depth frequency following Rodriguez-Iturbe and others (1999). Furthermore, Porporato and others (2003) observe that the mean of the exponential distribution of storm depth, χ [mm], is relatively uniform across the Kalahari rainfall gradient, whereas the mean of the exponential distribution of storm arrival frequency during the rainy season, ψ [d^{-1}] changes linearly ($r^2 = 0.99$; $n = 4$; $P < 0.01$) as a function of MAP. Therefore, ψ and χ are determined according to the results in Porporato and others (2003), so that $\psi = a \cdot MAP - b$ and $\chi = 11$, where $a = 4.3 \times 10^{-4}$ mm^{-1} d^{-1} and $b = 0.12$ d^{-1}. The resulting stochastic rainfall is used to determine daily rainfall for the rainy season (October–March) for any location along the Kalahari Transect given a MAP value. The annual rainfall distributions generated in this manner have excellent agreement with published estimates of the distribution of historical annual rainfall derived from station data (New and others 1999).

The necessary structural parameters for each of the sites along the Kalahari Transect are presented in Table 1 and Figure 2. Mean canopy cover, grass biomass [kg(grass) m(ground)$^{-2}$], grass-specific leaf area [m(grass)^2 kg(grass)$^{-1}$], and grass LAI [m(grass)^2 m(ground)$^{-2}$] are taken from published field results for the Kalahari Transect sites (Scholes and others 2002). To determine the site-average LAI, the volumetric distribution of woody vegetation leaf area is determined using a combination of field data and allometric relationships. The two-dimensional structure of canopies at each site is revealed using field observations of individual crown dimensions, and the vertical structure of canopies is generated using field observations of canopy height and average canopy depth. Leaf biomass and whole-tree biomass are estimated for each individual using generalized allometric relationships for southern African species developed by Goodman (1990), as revised by Dowty (1999). Field measurements of specific leaf area [m^2/kg] are used to calculate leaf area from each tree's allometrically determined leaf biomass. Each individual's leaf area is then distributed evenly throughout

the individual's canopy volume, to arrive at a leaf area per unit volume, or leaf area density [m^2/m^3]. Where canopy volumes intersect, leaf area density at intersecting locations is taken to be the sum of the contributing canopies' leaf area densities. Total site leaf area is the average of leaf area summed vertically. A field study examining the distribution of woody vegetation across the Kalahari Transect has shown that individuals have rather aggregated distributions at most sites (Caylor and others 2003). Therefore, we use detailed field observations of canopy structure to determine average leaf area. This method takes into account the relative amount of clumping of canopies and the overlap between adjacent canopies that may be caused by the aggregated distribution of individuals. At each of the Kalahari Transect sites, one thousand 1-year simulations are run to determine the changing nature of soil moisture under and between tree canopies across the rainfall gradient.

Results and Discussion

Recent analyses of spatial pattern in the Kalahari savannas have yielded new insights into the ways in which vegetation is organized across environmental gradients, from the distribution of individual trees observed in the field (Caylor and others 2003) to the variability in Normalized, Difference Vegetation, Index observed from space (Scanlon and others 2002). Savanna vegetation has a range of spatial patterns. In some regions, the mix of trees and grasses is heterogeneous, with patches of trees in a matrix of grass. In other locales, the trees are interspersed randomly (although some observers would say that their spacing is so regular as to be more uniform than random). The trees and grasses vary in biomass and height. The structural patterns of savannas can vary locally due to differences in soil moisture and nutrient availability. Alternatively, the same variations in structural patterns can be seen on the same soils as one moves regionally into wetter or drier precipitation regimes, as in the Kalahari Transect.

When our model is applied to determine the consequences of ecohydrological processes across the Kalahari Transect, regular patterns arise at the site level both at the nine study sites and across the Kalahari Transect as a whole. As an example of the higher-resolution local-site–level variation, Figure 3 shows a representative yearly simulation of the daily soil moisture under and between tree canopies at three representative sites along the transect. At Kataba, where the MAP is 879 mm, daily soil moisture is relatively high, and little relative difference is observed in soil moisture between and under canopies. When the interval between rains is longer, it can become somewhat drier between the tree canopies. At Sandveld, an intermediate site with MAP of 409 mm, consistent and relatively large differences are seen between the daily soil moisture conditions under and between tree canopies. Locations between tree canopies are almost always drier, usually to a substantial degree. At Vastrap, the southernmost site (216 mm MAP), differences between the soil moisture under and between canopies are negligible. For a few days at the end of the season in Vastrap, the soil moisture under the canopy is lower than the between-canopy value.

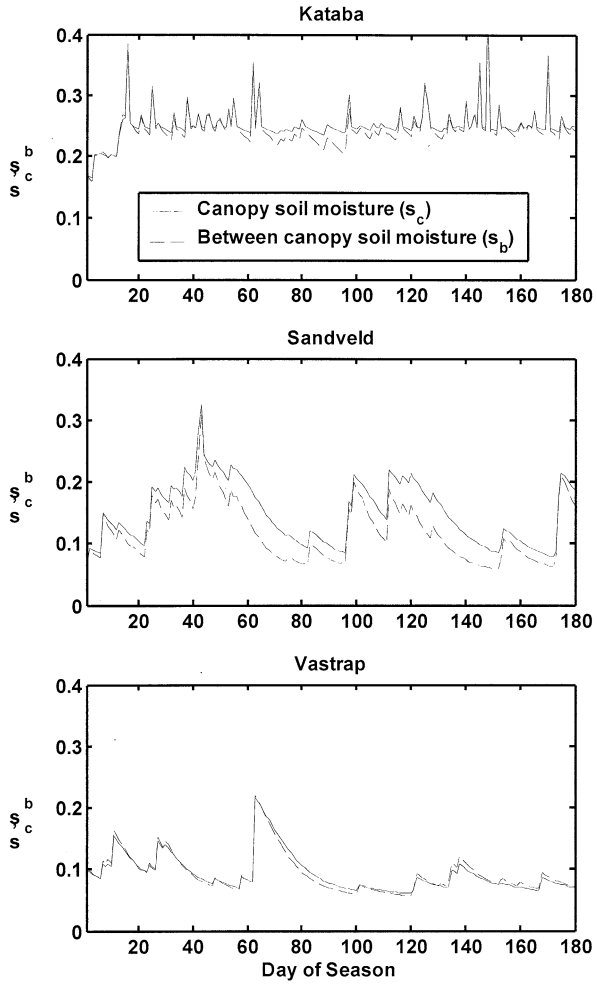

Figure 3. Daily soil moisture modeled under (s_c) and between (s_b) tree canopies at three sites across the Kalahari Transect. Minor difference is observed in soil moisture conditions at the northern and southern sites (Kataba and Vastrap), while large differences in soil moisture conditions occur at the intermediate site (Sandveld).

Changes in soil moisture under and below the tree canopies affect the distribution of stress-days for trees and grasses in the under-canopy and between-canopy portions of the landscape. The accumulated stress index ($\phi_{(x,y)}$) is highest for each vegetation component at the southernmost site and negligible at the northernmost site. The difference in soil stress conditions under and between canopies is measured by the difference in stress-days. The variation in vegetation stress under and between tree canopies is indexed using the stress thresholds for trees. The overall difference in stress levels at each site can then be determined by calculating the proportion of years during which the total number of stress-days in the between-canopy area exceeds the number of stress-days under the canopy.

As one traverses the rainfall gradient, changes in vegetation structure occur at both the patch and site scale. Mean tree biomass, tree cover, and tree LAI are seen to vary directly with rainfall (for example, tree cover and tree leaf area in Figure 2). In contrast to these general trends, the effect of large trees on the light and moisture environment is much more complex. The LAI of tree canopies reduces the amount of energy available under the canopy according to the model description provided above. At sites where canopy leaf area is higher, there is a greater reduction in incoming shortwave radiation available under the tree canopy. The reduced availability of incoming shortwave radiation affects subcanopy vegetation directly through energetic controls on transpiration and indirectly through reductions in bare soil evaporation. For all of the study sites, there are regular patterns in the percent reduction in shortwave radiation levels below tree canopies at each site and in the likelihood of reduced stress conditions under tree canopies over 1,000 simulations (Figure 4). At northern sites, there is little or no reduction in stress-days under tree canopies, but the canopies are seen to reduce incoming shortwave radiation levels up to 75%. At intermediate sites, the under-canopy vegetation almost always experiences fewer stress-days than the between-canopy areas. The effect of tree canopies on incoming shortwave radiation attenuation and water stress is reduced at the southern end of the transect.

The pattern in water stress under the tree canopies is such that reduced canopy stress occurs at sites in the middle of the transect (Figure 4). At the northern end of the transect, where MAP is high, the canopy has little effect on soil moisture stress levels, due to the high availability of soil moisture throughout the growing season. As MAP decreases,

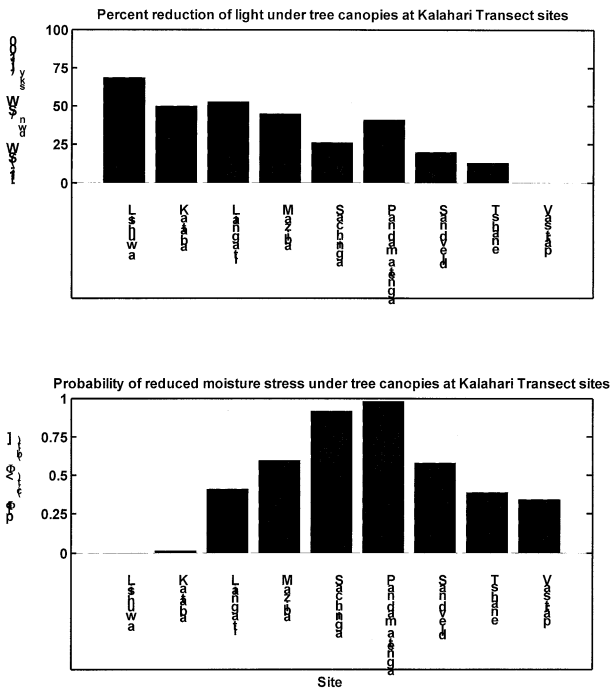

Figure 4. Changing light and water stress conditions under large tree canopies across the Kalahari Transect. The fraction of SW_{dwn} (incoming shortwave radiation below the canopy) relative to SW_{sky} (incoming shortwave radiation above and between the tree canopies) increases across the rainfall gradient from moist dry to, while the proportion of simulated years where soil moisture stress is lower under canopies than between canopies is greatest in the middle of the transect.

there is an increase in the proportion of years during which vegetation under the canopy experiences fewer total stress-days than the vegetation between the canopies. At sites where the proportion of years with reduced under canopy stress is greater than 0.5, the canopy is, on-average, less stressed than it is at the between-canopy locations.

Across the Kalahari Transect, the yearly difference in stress under and between canopies can be expressed as a relationship to the MAP for each simulation. Figure 5 illustrates the probability that the number of stress-days under tree canopies will be lower than the number of stress-days between canopies for grasses according to the deviation between a given year's rainfall and the long-term MAP across the latitudinal gradient. The probability surface is shown for ±2 SD of the MAP which represents 95% of the variation in MAP.

Linear distance-weighted interpolation between sites allows for a transectwide determination of how variation in rainfall might affect the relative stress levels between and under tree canopies. In the northernmost (wettest) sites, the model results

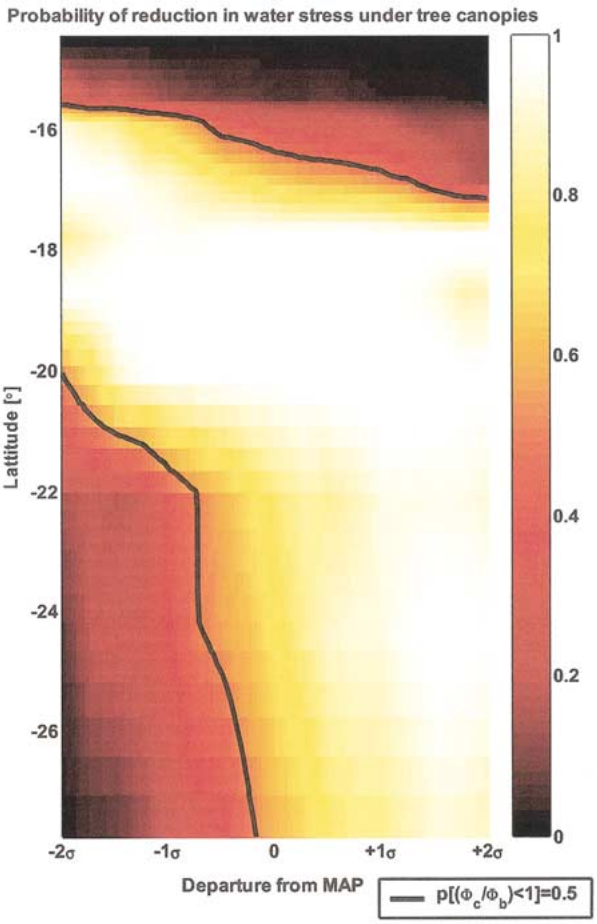

Figure 5. Probability of reduced water stress ($\Phi_c/\Phi_b < 1$) under tree canopies across the Kalahari Transect as a function of yearly deviation from MAP (-2σ to $+2\sigma$). Solid lines indicate 50% probability threshold.

indicate that there are no rainfall amounts within the ±2 SD MAP envelope that would lead to differences in water stress levels between and under tree canopies. A large central portion of the Kalahari Transect (from approximately16 to approximately 28°S) shows high probabilities of reduced stress under tree canopies for ±2 SD around the MAP value (Figure 5). At the northern part of this zone, canopy trees reduce stress in years with below-average precipitation (approximately 16–18°S); in the southern parts of the zone (approximately 20–28°S), tree canopies reduce water stress only during years with above-average precipitation.

A number of models of savanna ecosystem dynamics are based on cellular automata approaches that consider 'tree,' 'grass,' and 'bare' cells to be mutually exclusive (for example, van Wijk and Rodriguez-Iturbe 2002). The method presented here represents an alternative partitioning of the savanna spatial mosaic into 'below canopy' and 'between canopy.' Our model has simplified the complex spatial mosaic of savanna ecosystems in order to address the nature of tree canopy effects on a single variable—soil moisture—across a large rainfall gradient at a series of sites. The reduction of the savanna ecosystem into an essentially two-state system (under and between tree canopies) necessarily neglects the complex spatial patterns of individual tree distribution that arise in Kalahari Transect savannas (compare Caylor and others 2003). Nevertheless, we find that the consideration of canopy and between-canopy effects offers new insight into the ways in which structure and function are coupled in savanna ecosystems.

The water and energy balance approach is designed to minimize model complexity while maintaining important distinctions between the canopy and between-canopy environments across the Kalahari Transect rainfall gradient. In particular, a daily time step was chosen to capture the importance of stochastic rainfall events, and our analysis was limited to the growing season only. The limitation of our energy balance analysis to the period of consistently high air temperatures enables certain simplifying assumptions, including the use of a Priestley-Taylor potential evapotranspiration approach and a single parameter (C_G) to describe the contribution of soil heating to the overall energy budget. An approach that included subdaily time steps would further resolve the differences in the energy balance of the canopy and between-canopy environments, but it would require assumptions about the hourly distribution of rainfall and energy balance that cannot be supported by currently available data.

In addition, the approach presented here necessarily neglects some additional and possibly relevant components of soil water balance in savannas. In particular, the use of a single-layer bucket model of soil moisture does not allow for the action of hydraulic lift, which enables soil moisture to be transported upward in the soil column due to lower values of matric potential in drier upper layers. Obviously, the effect of hydraulic lift would be most important under tree canopies, where deep tree roots may enhance the passive transport of soil moisture upward in the soil column (Ludwig and others 2003). However, in this simulation, we assume equal rooting profiles for both trees and grass (that is, throughout the entire active rooting depth), so tree roots are unable to generate differences in soil moisture through hydraulic lift. In situations where pronounced differences are evi-

dent in tree versus grass rooting depth, we expect that such considerations would play a more important role in governing the spatial patterns of soil moisture stress in mixed tree and grass communities.

When considering vegetation comprised of a mixture of functional types of plants (Smith and others 1997), most ecologists are inclined to see the vegetation as a product of competition among the functional types to occupy the vegetation mosaic in a locale. One expects the plant functional type most suited to the environment to dominate other, less well-suited types. One example of this view applied within a modeling framework is the ECOSIEVE approach of Box (1981). In contrast to the expectation that competition should lead to the establishment of a single dominant functional group, this study indicates that the interactions among the functional types—tropical grasses and drought-deciduous trees—that codominate savannas are more complex.

Our model results indicate that tree canopies can have a significant local effect on the daily distribution of soil moisture (Figure 3) across a wide range of rainfall regimes. Climatic studies have shown that the Kalahari region tends to have periodic variation in rainfall over an 18-year cycle (Tyson 1986), and that annual rainfall amounts are also strongly governed by the magnitude and sign of El Nino–Southern Oscillation anomalies (Kogan 1998). In light of the known patterns of variability in rainfall over southern Africa, it is significant that both the magnitude and the sign of the effect of trees on other functional vegetation types (notably grasses) in the Kalahari region depends both on vegetation structure and the stochastic distributions of rainfall events (Figures 4 and 5). Although we have not attempted to simulate multi-year structural changes in vegetation composition and LAI, we note that the high degree of variability in water stress associated with the interannual variation in rainfall is likely to induce shifts in vegetation structure when prolonged periods of wet (or dry) regimes prevail. Studies of savannas in southern Texas have suggested that recent increases in tree cover were caused by a shift in rainfall seasonality during the late 1800s (Archer 1989). This finding and our model results provide some additional context for conceptualizing both historical and future structural changes in southern African savannas (Ringrose and others, 2002; Scanlon and others, 2002).

In addition to pronounced changes in tree–grass interaction across the Kalahari Transect rainfall gradient, our results show that this interaction can change in sign and magnitude over time in different parts of the transect. Given the pattern shown in Figure 5, the northern section of the Kalahari should be relatively invariant, with neutral effects of trees on the moisture environment beneath them. Further south, the effects of canopy trees on subcanopy soil moisture are likely to be positive for smaller plants growing beneath them. Still further south (below about 20°S), the trees have a positive effect on the soil moisture, but only in wet years. Therefore, in the southernmost section of the Kalahari, given the long cycles in wet and drought (Tyson and Crimp 1998), the potential mutualism of larger trees supplying regeneration sites of increased moisture in an overall dry environment turns on and off depending on the climate. Species adapted to regenerating and growing under trees would be advantaged in a wet decade and disadvantaged in a drier one. Of course, if the trees were absent, these rules would be different. Clearly, the interpretation of field observations and field experiments could easily be vexed by these effects. As an example, in an experimental study of a Tanzanian savanna (Ludwig and others 2001), the balance between positive and negative effects of large tree canopies on understory grass production was shown to vary between wet and dry seasons. Therefore, we suggest that in much of the southern part of the Kalahari Transect the rules for interaction could be expected to change in time, even at the same locations.

The high degree of control that vegetation structure exerts on the distribution of environmental resources (light and water) necessitates detailed characterization of vegetation structure to assess the potential effects of future and present environmental heterogeneity. In parts of the Kalahari Transect (or in different years for much of the transect), if trees successfully establish themselves after an ecological disturbance, there is a diversification of the regeneration niches either for other trees or for other plant functional types. In deforested areas, the absence of trees also implies a reduction in the diversity of regeneration site types. The simulated linkages between vegetation structure and water availability for both trees and grasses emphasize the importance of assessing the biophysical function of Kalahari savannas through ecohydrological techniques. We do not see the observations we have made here using a biophysical model of plant canopies as invalidating other theories so much as enriching them. Indeed, our conclusion that in semi-arid ecosystems tree canopy effects can be highly dependent on the extant climatic conditions — is supported by a number of

field observations (compare Belsky and others 1993; Ludwig and others 2001). Furthermore, the strong interactions between climate and vegetation in determining the spatial and temporal variability in soil moisture have been anticipated from a theoretical perspective (Rodriguez-Iturbe and others 1999). The unique Kalahari Transect, with its relatively similar deep sandy soil along a strong moisture gradient in a similar climatic regime, is central to the establishment and testing of the theory we have developed here.

ACKNOWLEDGMENTS

This study was part of the Southern African Regional Science Initiative (SAFARI 2000) and was conducted within the framework of the IGBP Kalahari Transect. K.K. C.'s research was supported by a NASA Earth System Science Fellowship while at the University of Virginia and by the Clayton Postdoctoral Fellowship at Princeton University. Additional funding was provided through the following NASA grants: NAG5-7956, NAG5-7266, NAG5-7862, and NAG5-9357. I.R.-I. acknowledges the support of the National Science Foundation through the grants in Biocomplexity (DEB-0083566) and the National Center for Earth-surface Dynamics (EAR-0120914). R. J. Scholes, P. R. Dowty, and the late D. A. B. Parsons helped to coordinate and conduct the fieldwork. We gratefully acknowledge the assistance of a number of people at the field sites, including Susan Ringrose (Pandamatenga), Otlogetse Totolo (Tshane), Mukufute Mukelabai (Kataba), Johannes Swanepoel (Sandveld), Evaristo Chileshe (Liangati, Lishuwa), Felix Bainga (Sachinga), Mwenda Mumbuna (Liangati), A. T. Mubone (Lishuwa), Petrus Rust (Vastrap), and the late W. Horn (Vastrap). K. Nomai was very helpful at Lishuwa, and we are grateful for his assistance. Finally, we thank Paolo D'Odorico, and three anonymous reviewers for their help with early drafts of the manuscript.

REFERENCES

Archer S. 1989. Have southern Texas savannas been converted to woodlands in recent history? Am Nat 134:545–61.

Atjay GL, Ketner P, Duvigneaud P. 1987. Terrestrial primary production and phytomass. In: Bolin B, Editor. The global carbon cycle. SCOPE 13. New York: Wiley. p 129–81.

Belsky AJ, Amundson RG, Duxbury JM, Riha SJ, Ali AR, Mwonga SM. 1989. The effects of trees on their physical, chemical and biological environments in a semi-arid savanna in Kenya. J Appl Ecol 26:1005–24.

Belsky AJ, Mwonga SM, Amundson RG, Duxbury JM, Ali AR. 1993. Comparative effects of isolated trees on their understory environments in high-and low-rainfall savannas. J Appl Ecol 30:143–55.

Bourliere F, Hadley M. 1970. The ecology of tropical savannas. Annu Rev Ecol Syst 1:125–52.

Boulet G, Chehbouni A, Braud I, Vauclin M, Haverkamp R, Zammit C. 2000. A simple water and energy balance model designed from regionalization and remote sensing data utilization. Agric Forest Meteorol 105:117–32.

Box, EO (1981). Macroclimate and plant forms: An introduction to predictive modeling in phytogeography. The Hague: W. Junk.

Breshears DD, Myers OB, Johnson SR, Meyer CW, Martens SN. 1997. Differential use of spatially heterogeneous soil moisture by two semiarid woody species: Pinus edulis and Juniperus monosperma. J Ecol 85:289–99.

Breshears D, Nyhan J, Heil C, Wilcox B. 1998. Effects of woody plants on microclimate in a semiarid woodland: soil temperature and evaporation in canopy and intercanopy patches. Int J Plant Sci 159:1010–17.

Breshears D, Barnes FJ. 1999. Interrelationships between plant functional types and soil moisture heterogeneity for semiarid landscapes within the grassland/forest continuum: a unified conceptual model. Landscape Ecol 14:465–78.

Brutsaert W. (1982). Evaporation into the atmosphere. Boston: D. Reidel.

Campbell GS, Norman JM. 1998. An introduction to environmental biophysics. New York: Springer-Verlag.

Caylor, KK, Dowty, PR, Shugart, HH, Ringrose, S. (2004) Vertical patterns of vegetation structure along the Kalahari Transect: the importance of spatial heterogeneity in modeling system productivity. Global Change Biol. 10(3):374–82.

Caylor KK, Shugart HH, Smith TM. 2003. Tree spacing along the Kalahari Transect. J Arid Environ 54(2):281–96.

Choudhury BJ, Idso SB, Reginato RJ. 1987. Analysis of an empirical model for soil heat flux under a growing wheat crop for estimating evaporation by an infrared-temperature based energy balance equation. Agric For Meteorol 39:283–97.

Coughenour MB. 1992. Spatial modeling and landscape characterization of an African pastoral ecosystem: a prototype model and its potential use for monitoring drought. In: McKenzie DH, Hyatt DE, McDonald VJ, Editors. Ecological indicators; vol 1. London: Elsevier Applied Science. p 787–810.

Darnell WL, Staylor WG, Ritchey NA, Gupta SK, Wilber AC. (1996). Surface radiation budget: a long-term global dataset of shortwave and longwave fluxes. EOS Trans Electron Suppl.

Dowty PR. (1999). Modeling Biophysical Processes in the Savannas of Southern Africa. [Dissertation]. Charlottesville: University of Virginia. 228 p.

Dowty PR, Caylor KK, Shugart HH, Emanuel WR. 2000. Approaches for the estimation of primary productivity and vegetation structure in the Kalahari region. In: Ringrose S, Chanda R, Editors. Towards sustainable natural resource management in the Kalahari Region. Gaborone: University of Botswana. p 287–304.

Eagleson PS, Segarra RI. 1985. Water-limited equilibrium of savanna vegetation systems. Water Resources Res 21:1483–93.

Fisher MJ, Rao IM, Ayarza MA, Lascano CE, Sanz JI, Thomas RJ, Vera RR. 1994. Carbon storage by introduced deep-rooted grasses in the South American savannas. Nature 371:236–38.

Gignoux J, Noble IR, Menaut JC. 1995. Modelling tree community dynamics in savannas: effects of competition with grasses and impact of disturbance. In: Bellan-Santini D, Bonin G, Emig C, editors. Functioning and dynamics of natural and perturbed Ecosystems. Paris: Lavoisier Intercept. p 219–30.

Goodman, PS. (1990). Soil, vegetation and large hebivore relations in Mkuzi Game Reserve, Natal. [dissertation]. Johannesburg (South Africa): University of the Witwatersrand.

Hipondoka MHT, Aranibar JN, Chirara C, Lihavha M, Macko SA. 2003. Vertical distribution of grass and tree roots in arid ecosystems of southern Africa niche differentiation of competition. J Arid Environ 54:319–25.

Huntley BJ, Walker BH. 1982. Ecology of tropical savannas. Berlin: Springer-Verlag.

Hutley LB, O'Grady AP, Eamus D. 2001. Monsoonal influences on evapotranspiration of savanna vegetation of northern Australia. Oecologia 126:434–43.

Idso SB, Aase JK, Jackson RD. 1975. Net radiation—soil heat flux relations as influenced by soil water content variations. Boundary Layer Meteorol 9:113–22.

Jackson NA, Wallace JS. 1999. Soil evaporation measurements in an agroforestry system in Kenya. Agric For Meteorol 94:203–15.

Jeltsch F, Milton S, Dean WRJ, VanRooyen N. 1996. Tree spacing and coexistence in semiarid savannas. J Ecol 84:583–95.

Jeltsch F, Milton SJ, Moloney KA. 1998. Modelling the impact of small-scale heterogeneities on tree–grass coexistence in semiarid savannas. J Ecol 86:780–93.

Jeltsch F, Weber GE, Grimm V. 2000. Ecological buffering mechanisms in savannas: a unifying theory of long-term tree–grass coexistences. Plant Ecol 161:161–71.

Joffre R, Rambal S. 1993. How tree cover influences the water balance of Mediterranean rangelands. Ecology 74:570–82.

Keya GA. 1997. Environmental triggers of germination and phenological events in an arid savannah region of northern Kenya. J Arid Environ 37:91–106.

Knoop WT, Walker BH. 1985. Interactions of woody and herbaceous vegetation in a southern African savanna. J Ecol 73:235–53.

Koch GW, Vitousek PM, Steffen WL, Walker BH. 1995. Terrestrial transects for global change research. Vegetatio 121: 53–65.

Kogan FN. 1998. A typical pattern of vegetation conditions in southern Africa during El Nino years detected from AVHRR data using three-channel numerical index. Int J Remote Sens 19:3689–95.

Kustas WP, Norman JM. 1997. A two-source approach for estimating turbulent fluxes using multiple angle thermal infrared observations. Water Resources Res 33:1495–508.

Laio F, Porporato A, Ridolfi L, Rodriguez-Iturbe I. 2001. Plants in water-controlled ecosystems: active role in hydrologic processes and response to water stress. II. Probabilistic soil moisture dynamics. Adv Water Resources 24:707–23.

Lhomme JP, Monteny B. 2000. Theoretical relationship between stomatal resistance and surface temperatures in sparse vegetation. Agric For Meteorol 104:119–31.

Lonsdale WM, Braithwaite PM, Farmer J. 1998. Modelling the recovery of an annual savanna grass following a fire-induced crash. Aust J Ecol 23:509–13.

Ludwig F, de Kroon H, Prins HHT, Berendse F. 2001. Effects of nutrients and shade on treegrass interactions in an East African savanna. J Veget Sci 12:579–88.

Ludwig F, Dawson TE, Kroon H, Berendse F, Prins HHT. 2003. Hydraulic lift in Acacia tortilis trees on an East African savanna. Oecologia 134(3):293–300.

McCown RL, Williams J. 1990. The water environment and implications for productivity. J Biogeog 17:513–20.

Menaut JC, Cesar J. 1979. Structure and primary productivity of Lamto savannas, Ivory Coast. Ecology 60:1197–210.

Mordelet P, Menaut JC. 1995. Influence of trees on aboveground production dynamics of grasses in a humid savanna. J Veget Sci 6:223–28.

New M, Hulme M, Jones P. 1999. Representing twentieth-century space–time climate variability. Part I. Development of a 1961–1990:(mean monthly terrestrial climatology. J Clim 12(3)829–56.

Phillips DL, MacMahon JA. 1981. Competition and spacing patterns in desert shrubs. J Ecol 69:97–115.

Porporato A, Laio F, Ridolfi L, Rodriguez-Iturbe I. 2001. Plants in water-controlled ecosystems: active role in hydrologic processes and response to water stress. III. Vegetation water stress. Adv Water Resources 24:725–44.

Porporato A, Laio F, Ridolfi L, Caylor KK, Rodriguez-Iturbe , I . 2003. Modeling the probability distribution function of soil moisture along the Kalahari Transect. J Geophys Res Atmospheres 108:(D3)4127–34.

Privette J, Tian Y, Roberts G, Scholes RJ, Wang Y, Caylor KK, Frost P. 2004. Structural characteristics and relationships of Kalahari woodlands and savannas. Global Change Biol. 10(3):281–91.

Ringrose S, Chipanshi AC, Matheson W, Chanda R, Motoma L, Magole I, Jellema A. 2002. Climate- and human-induced woody vegetation changes in Botswana and their implications for human adaptation. Environ Manage 30:98–109.

Rodriguez-Iturbe I, D'Odorico P, Porporato A, Ridolfi L. 1999. On the spatial and temporal links between vegetation, climate, and soil moisture. Water Resources Research 35:3709–22.

Sala OE, Laurenroth WK. 1982. Small rainfall events: an ecological role in semiarid regions. Oecologia 53:301–04.

Sarmiento G. 1984. The ecology of neotropical savannas. Harvard University Press. Cambridge: MA.

Scanlon TM, Albertson JD. 2004. Canopy scale measurements of CO_2 and water vapor exchange along a precipitation gradient in southern Africa. Global Change Biol. 10(3):329–41.

Scanlon TM, Albertson JD. 2003. The effects of water availability on the coupled land atmosphere exchange of CO_2, water, and energy over a heterogeneous surface. J Hydrometeorol. 4(5):789–809.

Scanlon TM, Albertson JD, Caylor KK, Williams C. 2002. Determining land surface fractional cover from NDVI and rainfall time series for a savanna ecosystem. Remote Sens Environ 82(23):376–88.

Scholes RJ, Dowty PR, Caylor KK, Parsons DAB, Frost PGH, Shugart HH. 2002. Trends in savanna structure and composition on an aridity gradient in the Kalahari. J Veget Sci 13:419–28.

Scholes RJ, Archer SR. 1997. Tree–grass interactions in savannas. Annu Rev Ecol Syst, 28:517–44.

Scholes RJ, Walker BH. 1993. An African savanna: synthesis of the Nylsvley study. Cambridge (UK): Cambridge University Press.

Simioni G, LeRoux X, Gignoux J, Sinoquet H. 2000. Treegrass: a 3D, process-based model for simulating plant interactions in tree–grass ecosystems. Ecol Model 131:47–63.

Skarpe C. 1990. Structure of the woody vegetation in disturbed and undisturbed arid savanna, Botswana. Vegetatio 87:11–18.

Smit GN, Rethman , NFG . 2000. The influence of tree thinning on the soil water in a semi-arid savanna of southern Africa. J Arid Environ 44:41–59.

Smith TM, Grant K. 1986. The role of competition in the spacing of trees in a Burkea africana Terminalia sericea savanna. Biotropica 18:219–23.

Smith TM, Goodman PS. 1987. Successional dynamics in an Acacia nilotica Euclea divinorum savannah in southern Africa. J Ecol 75:603–10.

Smith TM, Shugart HH, Woodward FI. 1997. Plant functional types: their relevance to ecosystem properties and global change. Cambridge (UK): Cambridge University Press.

Thomas DSG, Shaw PA. 1991. The Kalahari Environment. Cambridge (UK): Cambridge University Press.

Tothill JC, Mott JJ. 1985. Ecology and management of the world's savannas. Canberra: Australian Academy of Science. 384 pp.

Tyson PD. 1986. Climatic change and variability in southern Africa. Cape Town: Oxford University Press.

Tyson PD. The climate of the Kalahari Transect. Roy Soc S Afr 53:93–112.

Wijk MT, Rodriguez-Iturbe I. 2002. Treegrass competition in space and time: insights from a simple cellular automata model based on ecohydrological dynamics. Water Resources Res 38(9):1179–93.

Walter H. 1971. Ecology of tropical and subtropical vegetation. New York: Van Nostrand Reinhold Co.

Wilson TB, Witkowski ETF. 1998. Water requirements for germination and early seedling establishment in four African savanna woody plant species. J Arid Environ 38:541–50.

Yeaton RI, Cody ML. 1976. Competition and spacing in plant communities: the northern Mohave desert. J Ecol 64:689–96.